Journal Pre-proof

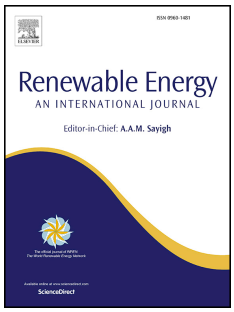

Small-scale autothermal thermochemical conversion of multiple solid biomass feedstock

Thomas Kirch, Paul R. Medwell, Cristian H. Birzer, Philip J. van Eyk

PII: S0960-1481(19)31617-9

DOI: https://doi.org/10.1016/j.renene.2019.10.120

Reference: RENE 12489

To appear in: *Renewable Energy*

Received Date: 30 January 2019

Revised Date: 11 July 2019

Accepted Date: 20 October 2019

Please cite this article as: Kirch T, Medwell PR, Birzer CH, van Eyk PJ, Small-scale autothermal thermochemical conversion of multiple solid biomass feedstock, *Renewable Energy* (2019), doi: https://doi.org/10.1016/j.renene.2019.10.120.

Small-Scale Autothermal Thermochemical Conversion of Multiple Solid Biomass Feedstock

Thomas Kirch[a,c,*], Paul R. Medwell[a,c], Cristian H. Birzer[a,c], Philip J. van Eyk[b,c]

[a] *School of Mechanical Engineering, The University of Adelaide, S.A. 5005, Australia*
[b] *School of Chemical Engineering, The University of Adelaide, S.A. 5005, Australia*
[c] *Humanitarian and Development Solutions Initiative, The University of Adelaide, South Australia 5005, Australia*

Abstract

The thermochemical conversion of four types of biomass in a batch-fed reverse downdraft process for heat generation in cookstoves is investigated. Fuel switching is widely considered inefficient because many combustion devices do not respond well to changes in fuel. Here, the use of agricultural by-products, represented by wheat straw, sheep manure, cow manure, and wood pellets is addressed. Two air supply rates within the oxygen-limited regime, where the fuel consumption is linearly dependent on the air supply, are investigated. At higher air supply rates, in the reaction-limited regime, low carbon yields lead to the exposure of the ash fraction to high temperatures, such that the resultant ash melting has detrimental effects on the process. Generally, no detrimental impact of the ash content on the conversion process within the oxygen-limited regime could be identified. The release of gaseous products, evaluated through cold gas efficiency, increases linearly from 24–54% with higher air flow, corresponding to increasing process temperatures from 690–980°C, and is largely fuel type independent. The char produced from all feedstocks fall within the highest classification for biochars, based on its elemental composition and determined by international protocols. This emphasises the potential of the investigated process for a combined production of producer gas and biochar from a variety of low-value biomass feedstocks.

Keywords:
Thermochemical conversion, Pyrolysis, Biomass, Gasification, Cookstove

Declarations of interest: none

*Corresponding author
Email address: thomas.kirch@adelaide.edu.au (Thomas Kirch)

1. Introduction

The difficulty with achieving fuel flexibility in any combustion system is evident even in highly advanced systems, such as internal combustion engines [30] and gas turbines [49]. These need to be adapted significantly to achieve acceptable efficiency when switching between different homogeneous fuels. This inherent difficulty is much more pronounced when using inhomogeneous solid fuels. However, it remains common practice for users of small-scale domestic combustion systems for cooking and heating to alternate their fuel source according to availability and/or season [63]. This includes nearly half the world's population who rely on such systems for basic survival [9]. In order to minimise adverse health and environmental implications of incomplete combustion, a deeper understanding of the combustion properties of a wide range of utilised fuels is necessary to enable more efficient combustor design for small-scale solid fuel systems.

Small-scale combustion systems that use a batch-fed autothermal reverse downdraft process, called gasifer stoves, have been shown to exhibit high potential to reduce emissions of incomplete combustion, compared with similar sized conventional systems [34, 48]. In these improved systems, the fuel batch is lit on its top surface, leading to the formation of a reaction front that moves in the opposite direction from the air supply down the fuel bed [12, 39]. The propagation velocity of the reaction front for a specific fuel is mainly dependent on the air supply. Three regimes are identified, dependent on the air flux, namely; the oxygen-limited regime, the reaction-limited regime, and the regime where the process is cooled by convection [17, 44, 21, 40, 41, 38, 56]. Increasing the air supply rate results in increasing process temperatures, which in turn influences the product composition of the thermochemical conversion in the reaction front. The products are a complex mixture of gases, liquids (forming an aerosol with the gases, called producer gas) and solid char, with increasing yields of gases and decreasing yields of liquids and char, at higher temperatures [16]. The aerosol which is produced is subsequently burned with secondary air for heat generation, while the char can be extracted at the end of the process [28, 29]. This process is widely used with limited understanding of the biomass conversion process and especially the influence of using various fuels with different compositions. Previously wood fuels and rice hulls have been studied [22, 23, 50, 54], however, a more comprehensive investigation with a variety of fuels is needed to provide insight of the key parameters and to influence future designs.

The need for an assessment of fuel types and characteristics for small-scale applications has previously been identified [53]. However, most previous investigations in comparable systems

have focussed on woody biomass [27, 23, 50, 51, 35, 32, 19, 33]. Other widely used fuels in practice include agricultural residues and animal manures, which are burned in great quantities per household in countries such as India [37], but have not been studied extensively. Generally, the appropriacy of manure as fuel is debatable since it reduces its availability as a fertiliser. In the autothermal reverse downdraft reactor, this effect is minimised because biochar is produced which can be used as an alternative soil amendment. Few studies have focussed on the use of manure as fuel [59, 3, 7]. High emissions have been reported for direct combustion [52], while the thermochemical conversion process has not specifically been addressed. Continuous downdraft gasification of cow manure has not been found feasible, because of the low heating value of the product gas and a satisfactory process could only be achieved when mixed with sawdust [45]. The use of agricultural residues, such as wheat straw, which are often disposed of by field burning [63, 43] could provide another widely available fuel source. Continuous gasification of straw has been indicated to only be possible with pelletised fuel, as chopped straw led to air blockages [20]. The main difference between woody biomass, agricultural residues and animal manures are the bulk density (depending on particle size and density), the ash content and the related energy density. While wood has a low ash content, it is greater in agricultural residues and is generally much higher in manure. The main topics discussed when dealing with high ash content fuels are melting, fusing and slag formation [61, 24]. It has been suggested that the high K and Si concentrations in straw ash could lead to slag formation [25], but when producing char the high unburned carbon concentrations and the integrity of the initial particle structures could minimise these possible effects. Therefore, general concerns with the use of high ash content fuels in thermochemical conversion processes do not necessarily apply to the presented system. The influence of a high ash content in fuels on the thermochemical conversion process and the quality and efficiency of combustible gas production is not well understood.

The combined production of char and clean-burning combustible gases could provide beneficial implications for the process as well as the environment. Not only can the solid char lower the concentration of tars in the producer gas and retain a large fraction of the ash [29] to reduce particulate emissions, the biochar is also a product that can be used for a variety of subsequent applications. The specific characteristics of the biochar, such as surface area and high carbon content, make it a particularly valuable for soil amendment purposes [62]. Biochar is widely produced in a variety of systems, such as earth pits or rotary kilns, where only a portion of the released volatile

products from the biomass feedstock are utilised to sustain the thermochemical conversion process and the remainder vented [10]. A process that combines the production of biochar with the full utilisation of the volatiles for heat generation could substantially increase the efficiency of the system. The quality of char produced from small-scale reverse downdraft gasification is seldom assessed though and needs further investigation for the application as a soil amendment, especially when utilising unconventional non-woody biomass feedstock.

The focus of this article is to assess various value biomass feedstocks for the combined production of producer gas and solid char in small-scale applications. Four fuels, namely wood pellets, wheat straw, sheep manure and cow manure, have been investigated at two air supply rates. The novelty of the paper is the insight of the producer gas composition and evolution in a small-scale batch-fed autothermal reverse downdraft system, with a specific focus on fuels with a high ash content. In contrast, similar papers typically omit measurements and analysis of the influences of the producer gas, instead looking only at the emissions from the subsequent combustion process. By isolating the products of the thermochemical conversion through the continuous measurement of the producer gas, the results are related to the main constituents of the supplied fuel and the produced char. These measurements enable an in-depth analysis of the thermochemical conversion process, the release of combustible products, as well as the quality of produced char. The analysis is extended for multiple fuels, with a wide range of ash contents. The resultant deeper understanding of the influence of biomass fuel composition, especially the ash content, on the autothermal thermochemical conversion process and its products, provides valuable information for downstream applications of the producer gas, as well as the char.

2. Materials and Methods

2.1. Reactor

The utilized small-scale thermochemical conversion and combustion reactor has been described previously [29]. Its main features, in the order of air flow are: an air supply chamber, a fuel grate on which the fuel rests, a reactor with ports for inserting thermocouples into the fuel bed, and a probe for the extraction of products above the fuel bed. Volatile products are combusted in a non-premixed flame, open to the environment, downstream of the extraction probe, however, the combustion process is not considered in this study.

Air is delivered at a constant flow rate during each of the experiments, resulting in the air mass flux specified in Table 1. The grate on which the fuel bed rests has 67.2% open area. The inner diameter of the reactor is 98 mm and is insulated with a 25-mm-thick thermal blanket. Eight K-type thermocouples (T1–T8) are situated along the length of the reactor. The entire device is placed on a weighing scale, Radwag WLC 20/A2, with a readability as well as repeatability of 10^{-4} kg and a maximum capacity of 20.0 kg.

The probe used to extract volatile products is situated at the top of the initial fuel bed. This probe is connected to a tar trap, which is used for the retention of all non-gaseous products. Subsequently, the gas sample is analysed, described in §2.2.

2.2. Gas Analyser

The gas stream was sampled with a MRU Vario Plus analyser. It measures CO_2, CO and CH_4 up to 30% (vol./vol.) and an accuracy $\pm$3% of the reading, using NDIR sensors. The measurements of O_2 and H_2 are measured with electrochemical sensors with a range up to 21% (vol./vol.) and an accuracy $\pm$0.2% of the absolute value, and a range up to 100% (vol./vol.) and an accuracy $\pm$0.02% of the reading, respectively. N_2 is determined by subtraction. The analyser was calibrated on a daily basis.

2.3. Fuels

Wood pellets, wheat straw, sheep manure and cow manure were tested in the present study. The results of the proximate and ultimate analyses for all fuels are presented in Figure 1. The ternary plots each enable the presentation of three constituents: (a) volatile matter (VM), fixed carbon (FC) and ash; and the three main elements: (b) carbon (C), hydrogen (H) and oxygen (O). Further information about the fuel and the tabulated values of the proximate and ultimate analyses are available in the Supplementary Material in Section S1.2. Due to the fuels bulk density 2.1 kg of wood pellets, 0.5 kg of wheat straw and 0.9 kg of manure were used for individual experiments.

2.4. Procedure

Prior to performing the experiments, the reactor was preheated and subsequent tests were started at inner reactor temperatures of $<$100 °C. Preheating was performed to avoid an influence from the large thermal mass of the reactor and reactor temperatures of $<$100 °C were chosen to minimise the influence of moisture evaporation when re-fuelling. Fuel was supplied in batches

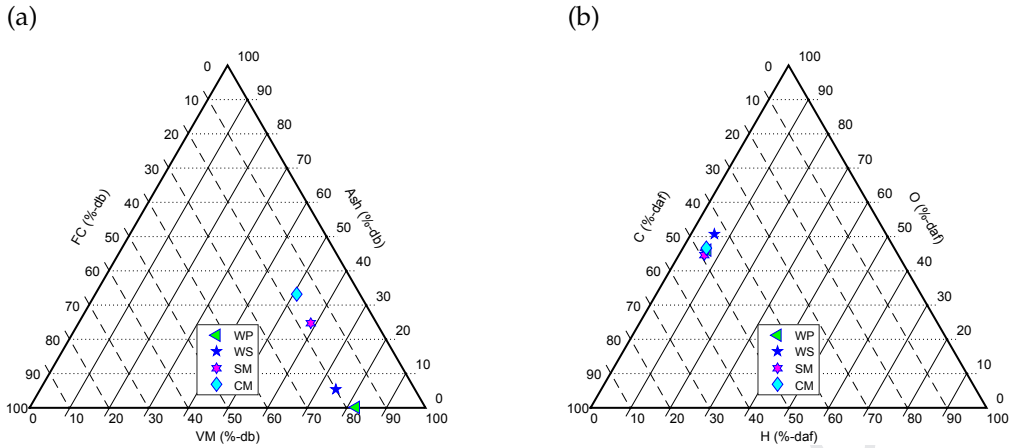

Figure 1: The fuel composition in terms of proximate analysis on a dry basis and ultimate analysis on a dry ash-free basis. The fuel types are: wood pellets (WP), wheat straw (WS), sheep manure (SM) and cow manure (CW). Axes show the three constituents of (a) the proximate analysis, fixed carbon (FC), ash, and volatile matter (VM), and (b) the ultimate analysis, carbon (C), oxygen (O), and hydrogen (H).

and the air mass flux was pre-set on the flow meters, prior to each experiment. Lighting was performed with the aid of 10 mL of methylated spirits (96% ethanol, CAS # 64-17-5) and a paper towel supplied to the top surface of the fuel bed. The temperature within the fuel bed was recorded throughout the process. The reaction front velocity for each configuration was determined in preliminary experiments (determined by the time taken between subsequent thermocouples reaching 600 °C) and the process was quenched once the reaction front reached the grate at the bottom of the fuel bed. Quenching was achieved by introducing ice water into the reactor from the top and by the provision of nitrogen (>99.99% N_2) instead of air to cool and prevent reactions inside the fuel bed. The remaining char was subsequently extracted. Multiple repeats for each tested fuel were performed at the two air supply rates, as presented in Figure 1. Air supply rates of 0.025 $kg \cdot m^{-2} \cdot s^{-1}$, for wood pellets, wheat straw and cow manure, and of 0.03 $kg \cdot m^{-2} \cdot s^{-1}$ for sheep manure, will be referred to herein as "low" and for all fuels 0.075 $kg \cdot m^{-2} \cdot s^{-1}$ as "high". These two air supply rates were chosen on the basis of preliminary experiments and a previous study [29], which have shown that these represent a high and low value within the oxygen limited regime. The exception of 0.030 $kg \cdot m^{-2} \cdot s^{-1}$ had to be made for sheep manure, since at lower flow rates no gaseous product measurements were possible, because excessive release of tar lead to repeated clogging of the tar trap.

Table 1: Experimental configurations, the number of repetitions performed and the experimental code.

Fuel type	Air Mass Flux ($kg \cdot m^{-2} \cdot s^{-1}$)	Repetitions	Code
Wood pellets	0.025	5	WP-L
	0.075	5	WP-H
Wheat straw	0.025	4	WS-L
	0.075	4	WS-H
Sheep manure	0.030	4	SM-L
	0.075	5	SM-H
Cow manure	0.025	3	CM-L
	0.075	4	CM-H

2.5. Analysis

For each experiment, the reactor is placed on a weighing scale to measure the fuel mass loss during the conversion process. The fuel mass loss was expected to display a linear profile with changes to air supply, based on previous research [40, 55]. The two air supplies at the focus of this study are 0.025 and 0.075 $kg \cdot m^{-2} \cdot s^{-1}$. These two flow rates were chosen on the basis of air supply regimes determined from mass loss measurements during preliminary experiments in the range 0.010–0.200 $kg \cdot m^{-2} \cdot s^{-1}$. Only mass loss was measured during the preliminary experiments, whilst gas sampling was performed during all subsequent tests. It should to be noted that comparable values found in the literature [41] are not based on weight measurements but calculated on the basis of thermocouple data, represented by the reaction front velocity and the fuel bulk density ($\dot{m}_{Fuel} = v_{Front} \cdot \rho_{Fuel}$). All figures presenting measured values include error bars that display the standard error of the mean [8].

Eight thermocouples recorded the gas phase temperature within the reactor. Mean maximum temperatures are determined as an average of the highest temperatures of the thermocouples T1–T7 and the value reported for each configuration was the mean of all repeat tests. Measurements of the lowest thermocouple T8 (at 20 mm from the fuel grate) were disregarded, since an increase of temperature due to the proximity to the fuel grate was observed.

An elemental balance was performed for carbon (C) and hydrogen (H) in the thermochemical conversion. The supply of N_2 via air was considered to be conserved, allowing the calculation of molecular C and H in the measured gas via the relationship between the supplied N_2 and the analysed N_2, as per Equation 1. Equations 2 and 3 present the overall calculation of molecular C and H in the measured gas, while the equations can be adapted for individual gas species. The

content of tars and water in the producer gas was not measured.

$$\dot{n}_{gas} = \frac{x_{gas}}{x_{N_2 measured}} \cdot \dot{n}_{N_2 air} \tag{1}$$

$$C_{gas} = \frac{m_{air} \cdot \omega_{N_{air}} / M_{N_2} \cdot (x_{CO_2} + x_{CO} + x_{CH_4}) / x_{N_2}}{(m_{fuel-daf} \cdot \omega_C - m_{char-af} \cdot \omega_C) / M_C} \tag{2}$$

$$H_{2_{gas}} = \frac{m_{air} \cdot \omega_{N_{air}} / M_{N_2} \cdot (x_{H_2} + 2 \cdot x_{CH_4}) / x_{N_2}}{(m_{fuel-daf} \cdot \omega_H - m_{char-af} \cdot \omega_H) / M_H} \tag{3}$$

Where $\dot{n}$ is the molecular gas flow and x is the molecular gas concentration. The provided or product mass is represented by m, the mass fraction by ω and the molecular mass by M.

To evaluate the process performance, the cold gas efficiency (CGE) was calculated on the basis of the energy content of the produced gases relative to the energy content of the converted fuel, as presented in Equation 4. The measured gas concentrations are considered as the energy content of the producer gas, while other hydrocarbon compounds and carbonaceous particles that might be released from the fuel bed are not included. The higher heating value (HHV) of the fuel and the char were measured using a bomb calorimeter and that of the gaseous species were based on well characterised values found in the literature [60].

$$CGE = \frac{V_{N2-air} / x_{N2} \cdot (x_{CO} \cdot 12.6 + x_{CH_4} \cdot 39.8 + x_{H_2} \cdot 12.8)}{HHV_{fuel} \cdot m_{fuel} - HHV_{char} \cdot m_{char}} \tag{4}$$

Fuels, as well as produced char samples from each configuration, were analysed for their ultimate (CHN), proximate (moisture (M), volatile matter (VM), fixed carbon (FC) and ash content) composition and their HHV. The proximate analysis was performed via thermogravimetric analysis (TGA), using a previously established method [47]. For both fuel and char samples, the ash content was also determined following ISO 18122:2015 [1] and the moisture content following ASTM D4442-92(2003) [4]. The reported proximate analyses therefore consist of the moisture content, via the ASTM standard, the VM fraction, via TGA analysis, the ash content, via the ISO standard, and the fixed carbon fraction is calculated via subtraction.

3. Results

3.1. Mass Flux and Process Temperature

Figure 2 shows the fuel mass flux—the consumption of fuel per time and reactor area—as a function of the supplied air mass flux, for each of the fuels considered in this study. Preliminary experiments were performed over a wide range of conditions, where only one repetition was performed. Also shown are the experimental results at the two air supply rates used for the majority of this work, as well as values found in the literature [41] for wood pellets. Previous research has shown that with increasing air flow, under sub-stoichiometric conditions, the fuel consumption increases initially linearly (oxygen-limited regime), then less severely until a further increase does not change the fuel consumption (reaction-limited regime) and at super-stoichiometric air supply, leads to cooling of the process until extinction (refer to §1). Cookstoves generally operate in the initial regime, where the fuel mass flux is linearly dependent on the air mass flux, and this regime is therefore the focus of the present study.

All fuels investigated behave similarly and the fuel mass flux increases linearly in the oxygen-limited regime in Figure 2 up to an air supply rate of $\approx$0.1 kg·m^{-2}·s^{-1}. In this regime, the value of the fuel mass flux (WP>WS>CM>SM) is notably lower when the fuel contains a high amount of ash. This lower fuel mass flux can be explained by a lower oxidiser-fuel contact, lower diffusion of gas species and the lower energy content of the bed, due to the high ash content, as hypothesised previously [40]. The lower fuel mass flux at a given air mass flux also results in a higher air to fuel ratio (A/F), which has previously been found to be similar for various biomass types with lower ash content [56]. This shows that the high ash content in manures has an impact on the conversion speed, but also that the conversion regimes are dependent on the superficial velocity (air mass flux / air density) and thus the oxygen availability as well as residence time.

For WP and WS, increasing the air mass flux to >0.1 kg·m^{-2}·s^{-1} leads to a transition to the reaction-limited regime and the fuel mass flux increases less rapidly with increasing air mass flux, until it reaches a plateau. For SM and CM, higher air flows exceeding >0.125 kg·m^{-2}·s^{-1} lead to a slight decrease in the fuel mass flux. This decrease is caused by a variety of factors including ash melting, which substantially alters the fuel bed properties. At such high air supply rates little to no char is produced. Therefore, the utilisation of this type of system outside the oxygen-limited regime is not advisable, as further discussed in Sections 3.3 and 3.4.

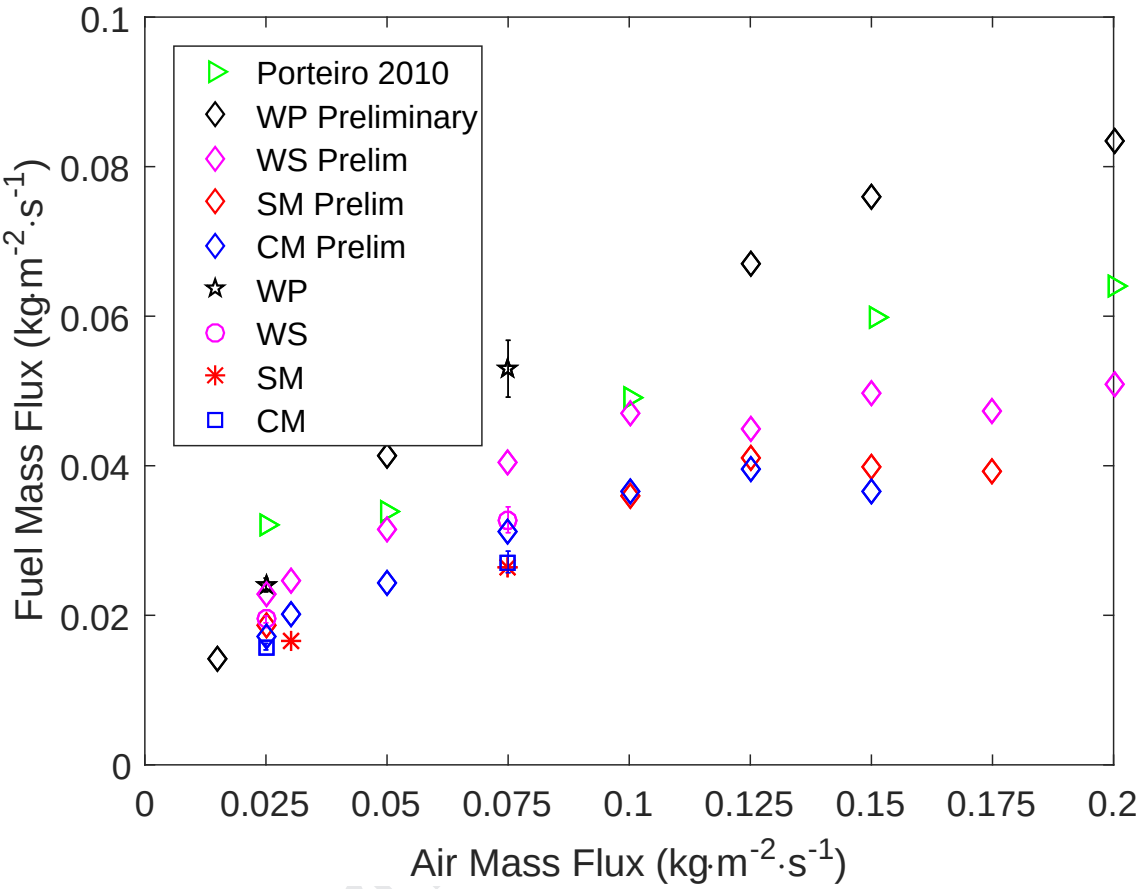

Figure 2: The fuel mass flux, the fuel consumption per time and reactor area, is presented as a function of the air mass flux for different experimental configurations, preliminary data and data found in the literature [41]. The error bars display the standard error of the mean.

The relationship between the mean peak temperature and the bulk density of the fuel bed is shown in Figure 3. The peak temperature is recorded at the centre of the fuel bed. It can be seen that there is a slight bulk density dependence of the mean peak temperature, similar to previous studies [40, 46]. With a lower bulk density, the total heat release per reactor volume is much lower and the thermal mass of the reactor wall and volume will have a greater influence on the peak temperature, compared with fuels with higher bulk density. Previously a higher bulk density has been related to a decreasing reaction front propagation velocity through the fuel bed [40], which also corresponds with a higher heat release per reactor volume. Here, no influence of other potentially related parameters, such as ash content, volatile matter content or particle size was

found.

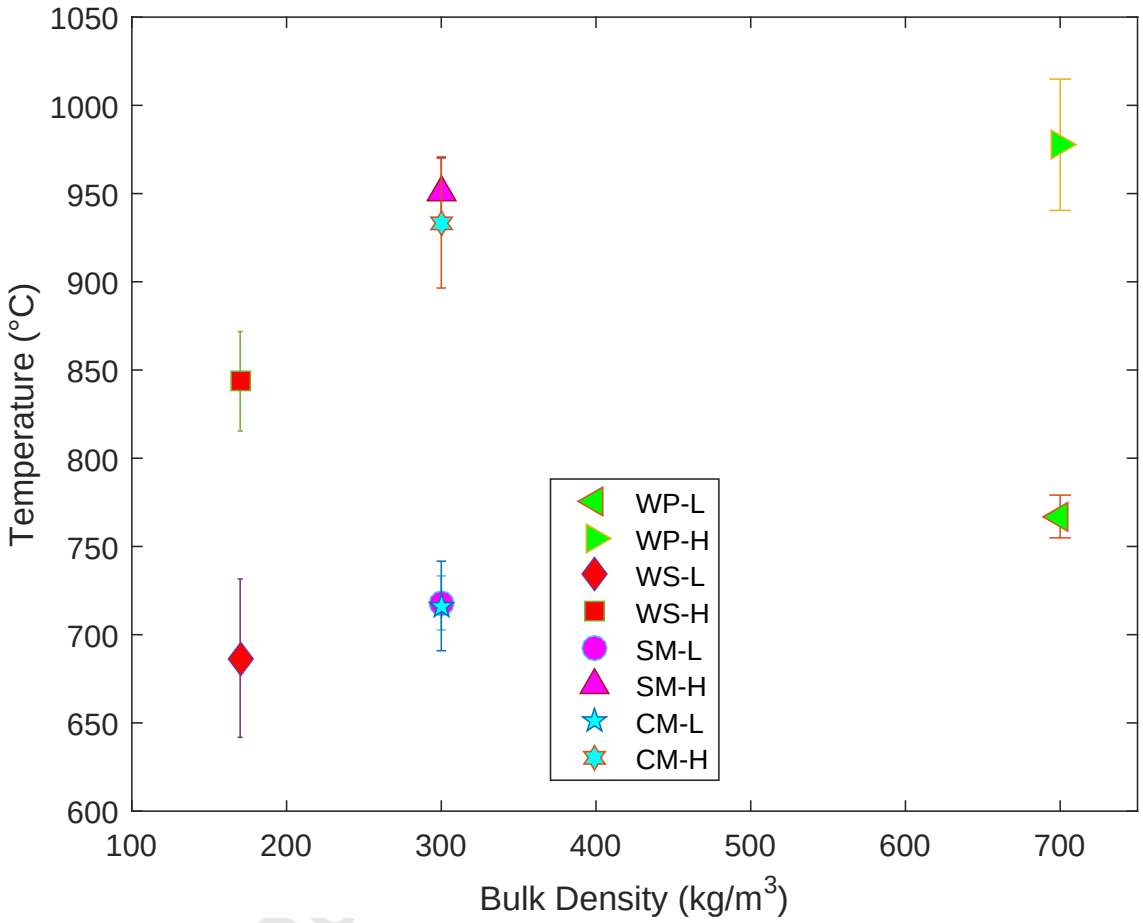

Figure 3: The mean peak conversion temperature at the reactor centre is presented in relation to the initial bulk density of the fuel. The error bars display the standard error of the mean.

3.2. *Gaseous Products*

The time-weighted average species concentration over the duration of the experiment, as well as the calculated HHV of the producer gases (refer to §2.5) are presented in Figure 4. The mean volumetric concentration of the main product species from the thermochemical conversion process and O_2 are shown for all four fuels at high and low air supply. It can be noted that for each configuration, the O_2 concentration is low and re-evaluation of the concentrations on a 0% O_2 basis did not change the trends in between configurations. In terms of application in small-scale

combustion systems, it needs to be kept in mind that the producer gas presented here is the fuel for the subsequent combustion process.

In Figure 4 it can be seen that increasing the air supply has contrary effects for CO_2 and CO. At higher air supply rates, less CO_2 and more CO is produced, which may be explained by a shift in the biomass conversion chemistry to an increasing primary product ratio of CO/CO_2 with increasing process temperatures [31]. Furthermore, previous research suggests that higher process temperatures [5] as well as higher temperatures in the char layer downstream of the reaction front [29] promote the conversion of tars (hydrocarbon compounds with higher boiling points than benzene [36]) to form mainly CO and H_2 (via reactions R13–R16, presented in the Supplementary Material in Table S3). This conversion of tars contributes to an increasing CO yield with greater air supply. As the combustible gases are more easily burned completely than the tars, greater conversion yields of these products may be beneficial for subsequent combustion.

Similar to the CO and CO_2 results, the hydrogen-containing species, H_2 and CH_4, also follow contrary trends with increased air flow rate. The mean H_2 concentration is higher with increasing air supply and process temperatures, while the CH_4 concentration decreases. This trend can be explained by a combination of the decomposition of hydrocarbon compounds at higher temperatures (R13–R16, see Supplementary Material in Table S3) and the interplay of homogeneous gasification reactions (R7–R12, see Supplementary Material in Table S3).

When comparing the different fuels with one another it can be seen that the highest concentrations of all combustible species is released from the WP, hence also exhibiting the highest HHV. CM exhibits the lowest HHV, while WS and SM are quite similar. Therefore, WP provides the highest quality gas for subsequent combustion. Whilst this supports the previous work that has focussed on woody biomass as a feedstock, it also highlights the challenges associated with the use of lower-grade fuels that are widely used.

In a previous study, wheat straw had been tested at an air supply of approximately $0.065 \mathrm{kg \cdot m^{-2} \cdot s^{-1}}$ and it was found that it exhibited a similar process temperature, but higher peak CO and CO_2 concentrations [25]. Although the previous system [25] is very similar to the one presented here, the comparison is limited because the char was consumed, leading to a higher prevalence of heterogeneous gasification reactions (R2–R5) and higher carbon oxide fractions in the producer gas. Similarly, higher temperatures and higher concentrations of all combustible gaseous products (CO, H_2 and CH_4), have been found with complete wheat straw fuel conversion elsewhere [61]. In

a similar, but continuous process, with char production, higher H_2 and CO concentrations were achieved with a simultaneous decrease in tars when using wood chips and wood pellets as fuel at 0.022 $kg \cdot m^{-2} \cdot s^{-1}$ [11]. In this continuous reactor the product gas passed through a constant layer of char at elevated temperatures [11], where tar cracking may occur, while here the char layer thickness increases as the reaction front propagates down the fuel bed and initially no char is present.

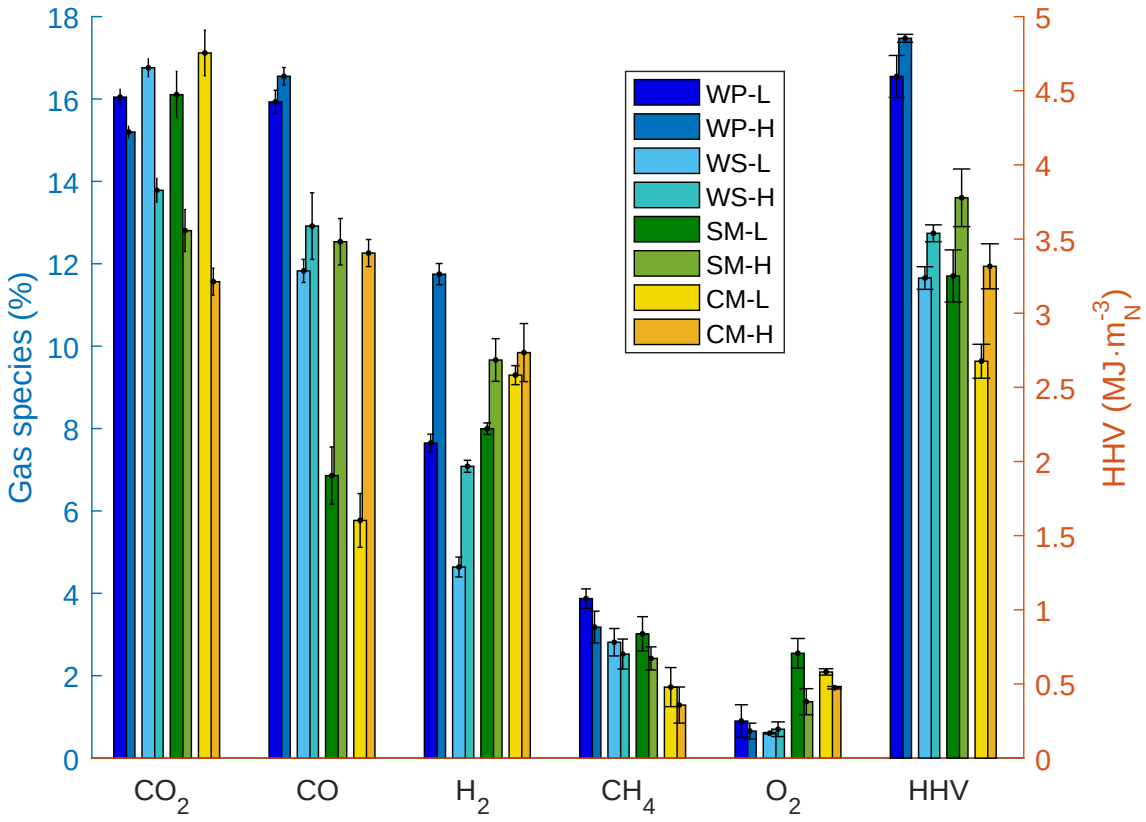

Figure 4: The time-weighted average volumetric producer gas composition, over the duration of the conversion process, as a mean of all replicates and the resulting HHV, of the gaseous products, are presented. The error bars display the standard error of the mean.

3.3. *Biomass Conversion*

The molecular conversion balance of carbon from the different fuels into the gaseous products, solid char and "other" (accounting mainly for tars and released particles) are presented in Figure 5. With increasing air flow, a general trend of increasing gaseous products accompanied by a

reduction of tars and char can be seen. This trend can be explained by higher process temperatures and has been well documented for biomass conversion processes [16, 6].

Focussing on a comparison of the conversion to permanent gases it can be seen that the combined yield of CO_2, CO and CH_4, at low flow rate follows the relation of WP > WS > CM > SM. At high air supply, the relation changes to CM > SM > WP > WS. The release of combustible gases, CO and CH_4, from the manures are particularly sensitive to changes in the air supply: from <40% at low air supply to >50% at high air supply. The higher increase of gas yield for the manures appears to be due to greater conversion of the fixed carbon fraction, with a simultaneous reduction of the char yield. For WP and WS both the char and other yields change more similarly, between low and high air supply. When considering that all fuels have a very similar carbon content, on a dry ash free basis (see Figure 1), the larger ash content in the manures appears to facilitate a greater conversion of fixed carbon to gaseous products at high air supply.

The char-carbon yield is lowest for the manures with high air flow. Thus, there will be less carbon available to form the structure of the char. This will be even more pronounced when further increasing the air supply, as described in Section 3.1. As char is a desired product of this process, a further increase of the air supply is not suitable for its production, especially when using manures as fuel—however, the higher proportion of producer gas in the high air supply case is advantageous.

The "other" fraction primarily includes tars, which are generally considered an undesirable product because they have been identified as a soot precursor for the subsequent combustion [18]. The fraction of tars is notably highest in SM, therefore explaining why this fuel was prone to clogging of the sampling line at $0.025\,kg{\cdot}m^{-2}{\cdot}s^{-1}$ and instead required an air supply of $0.030\,kg{\cdot}m^{-2}{\cdot}s^{-1}$ to ameliorate this issue (as described in §2.4). The lowest yields are achieved from WS, supporting the potential of this widely wasted fuel in this type of thermochemical conversion process.

Figure 6 presents the molecular balance of the supplied hydrogen in the fuel, into the measured gases and solid char, as well as "other", which accounts for mainly tars and water. For both air supply rates, WS presents the lowest conversion to gaseous products. It can be assumed that the low gas yield is due to lower peak process temperatures, when compared with the other fuels (see Figure 3). For both low and high air supply, it should also be noted that while the gas yields are similar for WP and SM, they are highest for CM. This trend cannot be explained by a temperature influence, as WP achieved the highest process temperature. Similar to the conversion

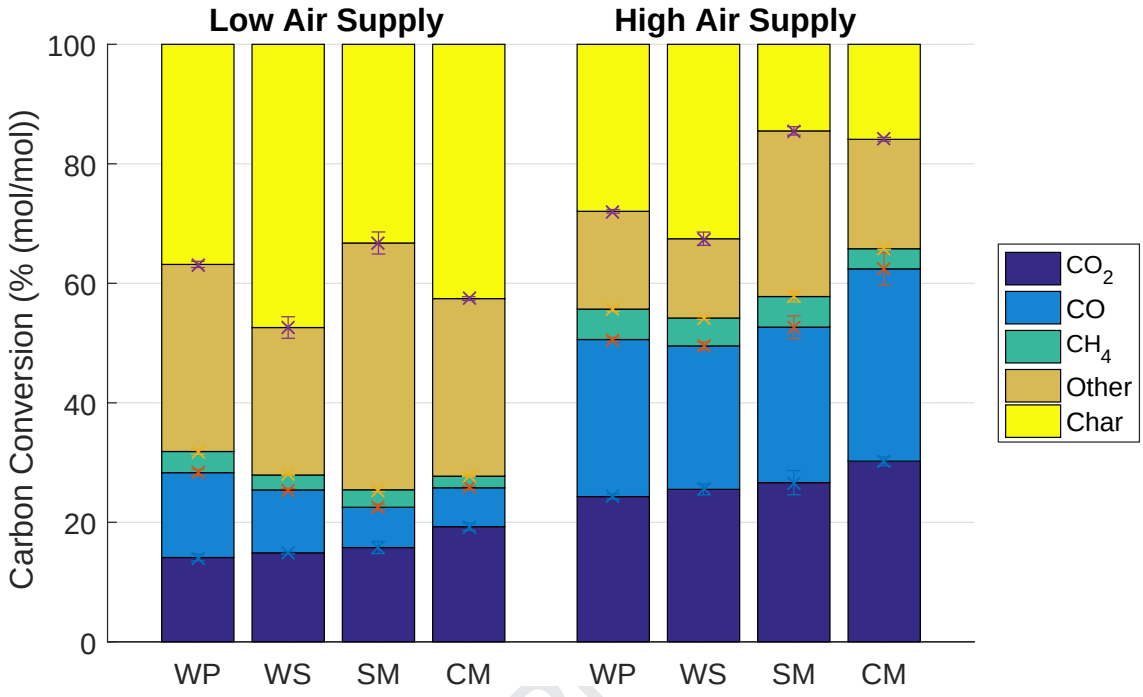

Figure 5: Conversion of fuel carbon to the gaseous products, CO_2, CO and CH_4, "other", accounting mainly for tars but also for carbonaceous particles that could be ejected from the fuel bed, and the solid char. The error bars display the standard error of the mean.

of carbon, the relatively high conversion yield of hydrogen-containing gases from the manures could be caused by the influence of the ash constituents. While the release of CH_4 appears to be consistent in between fuels at low and high air supply, the release of H_2 seems fuel dependent. This could be due to the presence of ash, since H_2 is highest in the manures.

The thermochemical conversion process can be evaluated through the cold gas efficiency (CGE), which provides a measure of the energy in the produced gas relative to that consumed from the supplied fuel (see §2.5). In Figure 7 the CGE is presented in relation to the mean peak process temperature. The efficiency appears to have a near-linear response with temperature, irrespective of fuel type.

In a similar-sized continuous downdraft gasifier using woody biomass pellets, at an air supply rate of ≈ 0.050 kg·m^{-2}·s^{-1}, a CGE of over 70% was reported [26]. Although, the peak process temperature is higher at 0.075 kg·m^{-2}·s^{-1}here and the producer gas composition appears similar, the CGE is more than 20% lower. Complete conversion of the char and a larger fraction of tars to

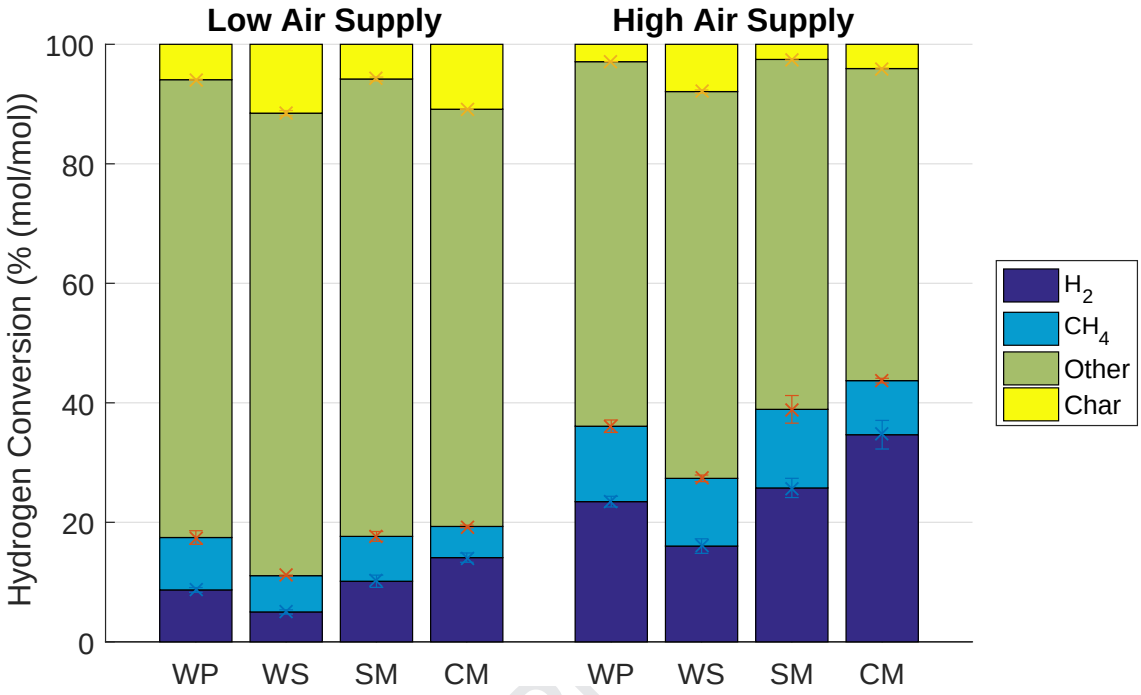

Figure 6: Conversion of fuel hydrogen to the gaseous products, H_2 and CH_4, "other", accounting mainly for water and tars, and the solid char. The error bars display the standard error of the mean.

producer gas in the continuous gasifier will contribute to this higher CGE.

3.4. Biochar

In Figure 8(a) the proximate-, and in 8(b) the ultimate-, analyses of the produced chars are shown as ternary plots (the respective values are provided in the Supplementary Material in Tables S4 and S5). The ternary plots enable the presentation of (a) the three constituents; volatile matter (VM), fixed carbon (FC) and ash; and (b) the three main elements: carbon (C), hydrogen (H) and oxygen (O).

The largest differences between the fuels can be seen in (a) along the fixed carbon and ash axes and in (b) along the carbon and oxygen axes. It can be noted that the carbon and the fixed carbon fractions generally decrease when increasing the air supply and are especially low for the manures. At 0.075 $kg{\cdot}m^{-2}{\cdot}s^{-1}$ only approximately 10% and 20% of fixed carbon remain in the char for CM and SM, respectively. At higher flow rates, the fixed carbon fraction is too low to retain a carbon structure, which is the basis of the char. Without the supporting carbon structure

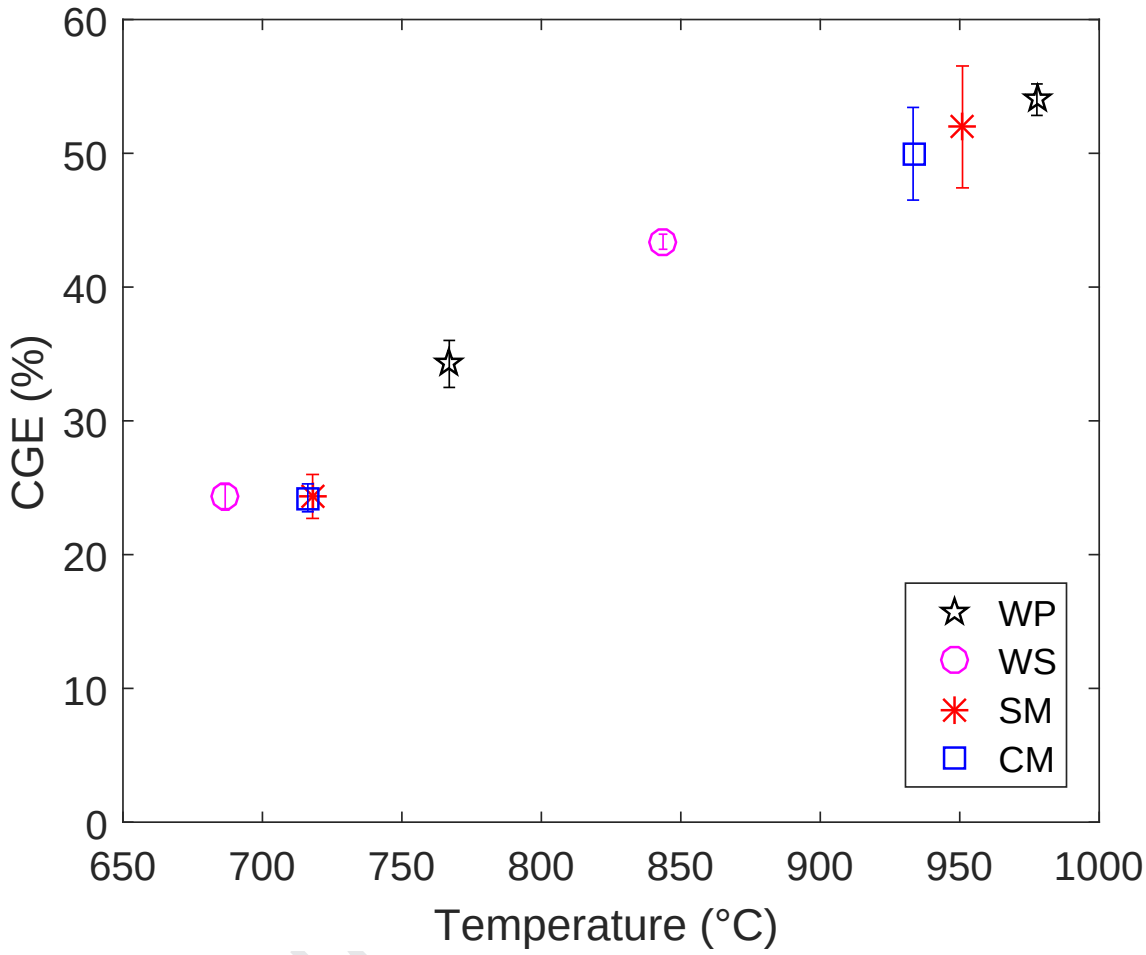

Figure 7: The cold gas efficiency (CGE) versus the mean peak temperature in the reaction front for all tested configurations. The error bars display the standard error of the mean.

and temperatures in excess of 900 °C (refer to Figure 3), ash melting occurs, which substantially alters the porous structure of the fuel bed and has negative process implications (refer to § 1). The impact of ash melting on the solid product can be seen in photographs which are included in the Supplementary Material in Figures S5 and S6.

Table 2 presents the higher heating value, the weight-based yield and the energy yield of the char. At low air supply for wood pellets, the char yield is 20% and the energy yield is 37%, which agree well with literature values under pyrolysis conditions of $\gtrsim$20% and $\gtrsim$40%, respectively [16, 62]. Similarly, wheat straw under low air supply conditions gives $\gtrsim$30% char yield and $\gtrsim$40%

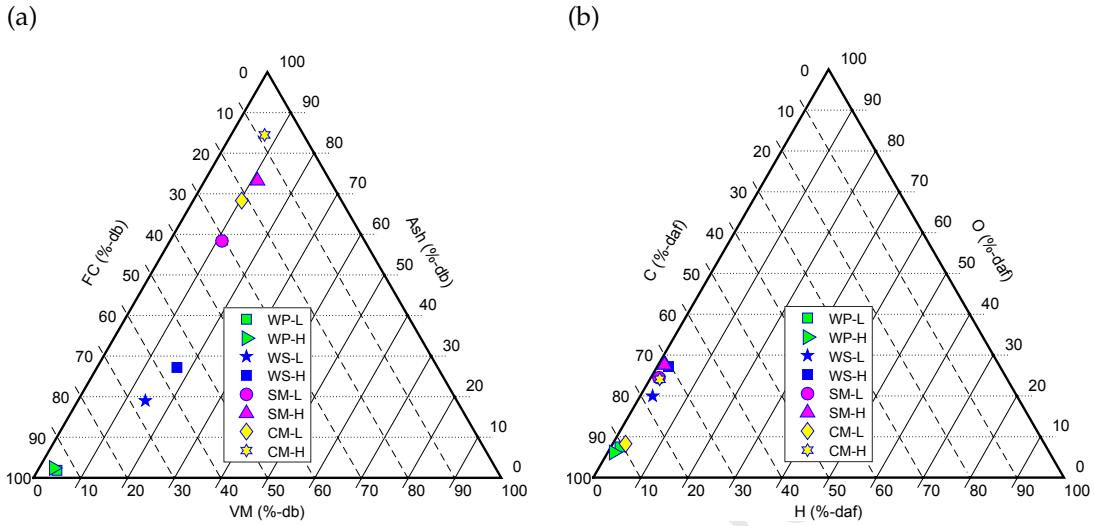

Figure 8: In (a) the proximate analyses, on a dry basis (db), and in (b) the ultimate analyses, on a dry ash free basis (daf), are presented. All values are on a mass basis.

energy yield in both Table 2 and pyrolysis literature [16, 62]. Therefore, the results indicate that at low air supply, pyrolysis conditions of temperatures >700°C are approached. In contrast, at higher air supply, the yields of both char and energy are lower by nearly a factor of two. Generally, it can be seen that increasing the air supply leads to a reduction in yields as well as heating value, because of the increasing ash fraction in the char.

Table 2: The mass yield (g/g), the energy yield (MJ/MJ) and the bulk calorific value (MJ/kg) of the produced char.

Air supply	WP	WS	SM	CM
Mass yield (g/g)				
low	0.20	0.32	0.40	0.50
high	0.14	0.24	0.31	0.37
Energy yield (MJ/MJ)				
low	0.37	0.44	0.33	0.39
high	0.26	0.27	0.21	0.12
HHV (MJ/kg)				
low	32.5	22.6	11.1	9.8
high	31.2	18.2	9.2	3.9

When considering a molecular balance, rather than a mass balance as presented by the proximate and ultimate analyses, generally a decrease of both the molecular H:C and O:C ratios has previously been identified with increasing process temperature, for woody biomass as well as

wheat straw [62] (H:C and O:C ratios for produced chars as well as the fuels are presented in the Supplementary Material in Figure S7). This trend can also be found in the present study and similarly applies to the SM and CM chars. The difference in O:C ratio, between the fuel and the char, is less severe in the case of the manures, as oxygen can be expected to be present within the ash [58]. All produced chars fall within the category of Class 1 biochars, based on their molecular composition, with H:C and O:C ratios lower than 0.7 and 0.4 respectively, as proposed by the European Biochar Foundation [2, 15] . Therefore, even the high ash content chars could attain the highest classification biochars for soil amendment purposes, but future work regarding further classification criteria will address this issue in more depth.

4. Discussion

As mentioned in Section 1, three regimes have been identified for the thermochemical conversion of many biomass materials with increasing air supply, namely: oxygen-limited, where the fuel conversion is linearly dependent on the air supply; reaction-limited, where the fuel conversion plateaus with respect to increasing air supply; and the regime where the process is cooled by convection. The present study focusses on the oxygen-limited regime, since char is mainly produced in this regime, however, preliminary experiments were also performed in the reaction-limited regime and the findings may aid in defining ongoing processes in these regimes more clearly.

When little oxygen is supplied to the ignited fuel, the conversion of the solid biomass is dominated by devolatilisation, leading to the formation of solid char (as defined by reaction R1 in the Supplementary Material in Table S3) with a lower influence of heterogeneous gasification reactions R2–R5 of the resultant char. When the air supply is increased, there is a general rise in fuel consumption, accompanied by higher process temperatures (see §3.1), higher yields of permanent gases and a reduction of the tar (see §3.3) and char yield (see §3.4), caused by a stronger influence of reactions R2–R5 (refer to the Supplementary Material in Table S3). This is supported by a comparison with the relevant literature reporting pyrolysis experiments [16, 62] (see §3.4), where similar char yields have been reported at comparable process temperatures for low air supply, while higher yields are reported at high air supply, when heterogeneous gasification reactions are more prominent if oxygen is supplied to the conversion process.

At low air supply, it should be noted that the molecular yield of C and H in the char is somewhat similar (interestingly WP and SM, and WS and CM, exhibit similar yields) while the reduction of yields at high air supply is more severe in the manures (see §3.3) compared with the lignocellulose fuels (WP and WS). Previously, it has been suggested that a higher lignin content, the most stable lignocellulose component, promotes the formation of char during pyrolysis [13]. While this will contribute to a similar carbon conversion yield of char for WP and WS, which generally have a similar lignin content [57], the fraction in manures is generally very low [42]. Furthermore, it is shown that the duration of the conversion per unit mass of supplied fuel was very similar for all fuels, although in the case of the high ash content fuels, much less dry ash-free fuel is available (see §3.2). This shows that the dry ash-free conversion process occurs more slowly in high ash content fuels but a larger fraction of the FC is consumed, leading to nearly complete conversion of FC under oxygen-limited conditions.

In the manure and WS chars for high and low air supply rates, more than 50% and 20% (g/g), respectively, of the product is ash. This ash is retained in the solid structure which minimises the influence of elutriation or ash melting, from these high ash containing fuels. In all cases, even for CM at high air supply where the char contains only 10% (g/g) FC (see §3.4), the carbon structure largely remains but loose ash can be noticed on the char surface (refer to the Supplementary Material in Figure S5). This shows that through the production of the char, not only is a valuable solid (see §3.4) created, but also beneficial process implications are achieved. Furthermore, the clear separation of a devolatilisation and a char conversion phase, which becomes less pronounced as lower char yields are achieved, will cease at higher air supply rates for high ash content fuels.

The high ash content in the manures does not appear to have a negative influence on the conversion to permanent gases, within the oxygen-limited regime (see §3.3). The presence of char has previously been shown to increase tar conversion to permanent gases [29] (as per reactions R13–R16, see Supplementary Material in Table S3). While this influence has not specifically been studied for chars with a high ash content, it can be assumed to be influential on the release of gaseous products. Overall, the molecular conversion to permanent gases and its evaluation through the CGE, appears to be mostly process temperature dependent, while the fuel type plays a secondary role.

In the reaction-limited regime, the conversion reactions of biomass devolatilisation and heterogeneous gasification of the produced char body (R1–R5, see Supplementary Material in Ta-

ble S3) occur more concurrently. This leads to a more simultaneous conversion and release of the volatile matter and fixed carbon fractions from the fuel batch. For all fuels, this causes a substantial reduction in the char yield and a change in bed morphology. The absence of the char structure at high air supplies leads to ash either being expelled in the form of fly-ash or exposed to high process temperatures exceeding the ash melting point [14] leading to product melting and particle fusing, which alters the fuel bed properties and causes problems within the reactor (refer to the Supplementary Material in Figures S5 and S6). This is of little importance for low-ash fuels but can be detrimental to high-ash fuels, such as manures. Problems occurring in the reactor include channel forming, which changes the combustion characteristic from a near homogeneous reaction front to locally differing conversion conditions, or ash fusing to walls. Furthermore, the plateau of the fuel conversion with a simultaneous increase of the air supply, in the reaction-limited regime, leads to increased dilution of combustible products.

5. Conclusions

The presented study investigates the conversion behaviour of four different biomass fuels in an autothermal reverse downdraft process, which is often used in gasifier cookstoves. The influence of two air supplies on the biomass conversion within the oxygen-limited regime, where the fuel conversion is linearly dependent on the air supply, is the focus of this study. Process implications of higher air supplies are also addressed.

- The conversion behaviour is similar for all fuels, irrespective of the ash-content, but the fuel conversion is inversely proportional to the ash-content.
- With increasing air supply and increasing process temperatures more fuel carbon is consumed and the possibility of ash-melting increases. By limiting the air supply, where more char is produced and peak temperatures are lower, ash-melting can be avoided.
- The fuel conversion to gaseous products in the oxygen-limited regime is mainly temperature dependent and independent of fuel type. Thus gaseous product estimation from this process could be based on the peak process temperatures.
- All produced chars achieve the highest classification, through international protocols, for soil amendment purposes, based on their elemental composition.

Overall, it is shown that the thermochemical conversion of a high value biomass fuel, wood pellets, exhibit the best performance, but similar results can be achieved even with the lowest value biomass fuels, manures, and the agricultural by-product, wheat straw. The issue of ash melting and fusing, which is often detrimental to traditional combustion of high ash-content fuels can be avoided here through limitation of the air supply and the production of char. This highlights the potential for utilisation of low value fuels in the presented system for a combined production of producer gas for heat generation and biochar for soil amendment applications.

6. Acknowledgements

The authors wish to acknowledge the support of The University of Adelaide and Marc Simpson, the laboratory facilities manager. The support provided by the Studienstiftung des Deutschen Volkes is also gratefully acknowledged.

7. References

[1] , 2015. ISO 18122:2015 Solid biofuels - Determination of ash content.

[2] , 2015. Standardized Product Definition and Product Testing Guidelines for Biochar That Is Used in Soil. International Biochar Initiative, 61.

[3] Abeliotis, K., Pakula, C., 2013. Reducing health impacts of biomass burning for cooking-the need for cookstove performance testing. Energy Efficiency 6 (3), 585–594.

[4] American Society for Testing and Materials, 2003. ASTM D4442-92(2003): Standard Test Methods for Direct Moisture Content Measurement of Wood and Wood-based Materials.

[5] Baker, E., Brown, M., Elliott, D. C., Mudge, L., 1988. Characterization and treatment of tars from biomass gasifiers. AIChE 1988 Summer National Meeting, 11.

[6] Basu, P., 2013. Gasification Theory. In: Biomass Gasification, Pyrolysis and Torrefaction. Elsevier Inc., Ch. 7, pp. 199–248.

[7] Birzer, C., Medwell, P., MacFarlane, G., Read, M., Wilkey, J., Higgins, M., West, T., 2014. A Biochar-producing, Dung-burning Cookstove for Humanitarian Purposes. Procedia Engineering 78, 243–249.

[8] Bondy, W. H., Zlot, W., 1976. The Standard Error of the Mean and the Difference between Means for Finite Populations. The American Statistician 30 (2), 96–97.

[9] Bonjour, S., Adair-Rohani, H., Wolf, J., Bruce, N. G., Mehta, S., Prüss-Ustün, A., Lahiff, M., Rehfuess, E. A., Mishra, V., Smith, K. R., 2013. Solid fuel use for household cooking: Country and regional estimates for 1980-2010. Environmental Health Perspectives 121 (7), 784–790.

[10] Brewer, C. E., Brown, R. C., 2012. Biochar. In: Comprehensive Renewable Energy. Elsevier Ltd., Ch. 5, pp. 357–384.

[11] Daouk, E., Van de Steene, L., Paviet, F., Martin, E., Valette, J., Salvador, S., 2017. Oxidative pyrolysis of wood chips and of wood pellets in a downdraft continuous fixed bed reactor. Fuel 196, 408–418.

[12] Dasappa, S., 2014. Thermochemical Conversion of Biomass. In: Hornung, A. (Ed.), Transformation of Biomass: Theory to Practice. JohnWiley & Sons, Ltd, Ch. 6, pp. 133–157.

[13] Dorez, G., Ferry, L., Sonnier, R., Taguet, A., Lopez-Cuesta, J. M., 2014. Effect of cellulose, hemicellulose and lignin contents on pyrolysis and combustion of natural fibers. Journal of Analytical and Applied Pyrolysis 107, 323–331.

[14] Du, S., Yang, H., Qian, K., Wang, X., Chen, H., 2014. Fusion and transformation properties of the inorganic components in biomass ash. Fuel 117, 1281–1287.

[15] EBC (2012), 2017. European Biochar Certificate - GuidelinesGuidelines for a Sustainable Production of Biochar. Tech. rep., European Biochar Foundation (EBC), Arbaz, Switzerland.

[16] Fagbemi, L., Khezami, L., Capart, R., 2001. Pyrolysis products from different biomasses. Applied Energy 69 (4), 293–306.

[17] Fatehi, M., Kaviany, M., 1994. Adiabatic reverse combustion in a packed bed. Combustion and Flame 99 (1), 1–17.

[18] Fitzpatrick, E. M., Bartle, K. D., Kubacki, M. L., Jones, J. M., Pourkashanian, M., Ross, A. B., Williams, A., Kubica, K., 2009. The mechanism of the formation of soot and other pollutants during the co-firing of coal and pine wood in a fixed bed combustor. Fuel 88 (12), 2409–2417.

[19] González, W. A., Pérez, J. F., Chapela, S., Porteiro, J., 2018. Numerical analysis of wood biomass packing factor in a fixed-bed gasification process. Renewable Energy 121, 579–589.

[20] Henrich, E., Dinjus, E., Rumpel, S., Stahl, R., 2001. A Two-Stage Pyrolysis/Gasification Process for Herbaceous Waste Biomass from Agriculture. In: Bridgwater, A. (Ed.), Progress in Thermochemical Biomass Conversion. Blackwell Science Ltd, Bodmin, pp. 221–236.

[21] Horttanainen, M., Saastamoinen, J., Sarkomaa, P., 2002. Operational limits of ignition front propagation against airflow in packed beds of different wood fuels. Energy & Fuels 16 (3), 676–686.

[22] James R., A., Yuan, W., Boyette, M., 2016. The Effect of Biomass Physical Properties on Top-Lit Updraft Gasification of Woodchips. Energies 9 (4), 283.

[23] James R, A. M., Yuan, W., Boyette, M. D., Wang, D., 2018. Airflow and insulation effects on simultaneous syngas and biochar production in a top-lit updraft biomass gasifier. Renewable Energy 117, 116–124.

[24] Jones, J. M., Lea-Langton, A. R., Ma, L., Pourkashanian, M., Williams, A., 2014. Pollutants Generated by the Combustion of Solid Biomass Fuels. Springer London Heidelberg New York Dordrecht.

[25] Khor, A., Ryu, C., bin Yang, Y., Sharifi, V. N., Swithenbank, J., 2007. Straw combustion in a fixed bed combustor. Fuel 86 (1-2), 152–160.

[26] Kihedu, J. H., Yoshiie, R., Nunome, Y., Ueki, Y., Naruse, I., 2014. Counter-flow air gasification of woody biomass pellets in the auto-thermal packed bed reactor. Fuel 117, 1242–1247.

[27] Kirch, T., Birzer, C. H., Eyk, P. J. V., Medwell, P. R., 2018. Influence of Primary and Secondary Air Supply on Gaseous Emissions from a Small-Scale Staged Solid Biomass Fuel Combustor. Energy & Fuels 32, 4212–4220.

[28] Kirch, T., Medwell, P. R., Birzer, C. H., 2016. Natural draft and forced primary air combustion properties of a top-lit up-draft research furnace. Biomass and Bioenergy 91, 108–115.

[29] Kirch, T., Medwell, P. R., Birzer, C. H., Van Eyk, P. J., 2018. Influences of fuel bed depth and air supply on small-scale batch-fed reverse downdraft biomass conversion. Energy & Fuels 32, 8507–8518.

[30] Klimstra, J., 2015. Fuel flexibility with dual-fuel engines. In: Oakey, J. (Ed.), Fuel Flexible Energy Generation: Solid, Liquid and Gaseous Fuels. Elsevier Ltd, pp. 293–304.

[31] Laurendeau, N. M., 1978. Heterogeneous kinetics of coal char gasification and combustion. Progress in Energy and Combustion Science 4 (4), 221–270.

[32] Lenis, Y. A., Osorio, L. F., Pérez, J. F., 2013. Fixed bed gasification of wood species with potential as energy crops in Colombia: The effect of the physicochemical properties. Energy Sources, Part A: Recovery, Utilization and Environmental Effects 35 (17), 1608–1617.

[33] Lenis, Y. A., Pérez, J. F., Melgar, A., 2016. Fixed bed gasification of Jacaranda Copaia wood: Effect of packing factor and oxygen enriched air. Industrial Crops and Products 84, 166–175.

[34] MacCarty, N., Still, D., Ogle, D., 2010. Fuel use and emissions performance of fifty cooking stoves in the laboratory and related benchmarks of performance. Energy for Sustainable Development 14 (3), 161–171.

[35] Mahapatra, S., Kumar, S., Dasappa, S., 2016. Gasification of wood particles in a co-current packed bed: Experiments and model analysis. Fuel Processing Technology 145, 76–89.

[36] Milne, T. A., Evans, R. J., Abatzoglou, N., 1998. Biomass Gasifier "Tars": Their Nature , Formation , and Conversion. National Technical Information Service (NTIS), 1–68.

[37] Mukunda, H. S., Dasappa, S., Paul, P. J., Rajan, N. K. S., Yagnaraman, M., Ravi Kumar, D., Deogaonkar, M., 2010. Gasifier stoves - science, technology and field outreach. Current Science 98 (5), 627–638.

[38] Pérez, J. F., Melgar, A., Benjumea, P. N., 2012. Effect of operating and design parameters on the gasification/combustion process of waste biomass in fixed bed downdraft reactors: An experimental study. Fuel 96, 487–496.

[39] Pham, X. H., Piriou, B., Salvador, S., Valette, J., Van de Steene, L., 2018. Oxidative pyrolysis of pine wood, wheat straw and miscanthus pellets in a fixed bed. Fuel Processing Technology 178 (June), 226–235.

[40] Porteiro, J., Patiño, D., Collazo, J., Granada, E., Moran, J., Miguez, J. L., 2010. Experimental analysis of the ignition front propagation of several biomass fuels in a fixed-bed combustor. Fuel 89 (1), 26–35.

[41] Porteiro, J., Patiño, D., Moran, J., Granada, E., 2010. Study of a fixed-bed biomass combustor: Influential parameters on ignition front propagation using parametric analysis. Energy & Fuels 24 (7), 3890–3897.

[42] Prasad, S., Singh, A., Joshi, H. C., 2007. Ethanol as an alternative fuel from agricultural, industrial and urban residues. Resources, Conservation and Recycling 50 (1), 1–39.

[43] Rajput, P., Sarin, M. M., 2014. Polar and non-polar organic aerosols from large-scale agricultural-waste burning emissions in Northern India: Implications to organic mass-to-organic carbon ratio. Chemosphere 103, 74–79.

[44] Rönnbäck, M., Axell, M., Gustavsson, L., Thunman, H., Lecher, B., 2001. Combustion processes in a biomass fuel bed - Experimental results. In: Bridgwater, A. (Ed.), Progress in Thermochemical Biomass Conversion. Blackwell Science Ltd, Bodmin, Ch. 59, pp. 743–757.

[45] Roy, P. C., Datta, A., Chakraborty, N., 2010. Assessment of cow dung as a supplementary fuel in a downdraft biomass gasifier. Renewable Energy 35 (2), 379–386.

[46] Sakthivadivel, D., Iniyan, S., 2017. Combustion characteristics of biomass fuels in a fixed bed micro-gasifier cook stove. Journal of Mechanical Science and Technology 31 (2), 995–1002.

[47] Saldarriaga, J. F., Aguado, R., Pablos, A., Amutio, M., Olazar, M., Bilbao, J., 2015. Fast characterization of biomass fuels by thermogravimetric analysis (TGA). Fuel 140, 744–751.

[48] Sutar, K. B., Kohli, S., Ravi, M. R., Ray, A., 2015. Biomass cookstoves : A review of technical aspects. Renewable and Sustainable Energy Reviews 41, 1128–1166.

[49] Taamallah, S., Vogiatzaki, K., Alzahrani, F. M., Mokheimer, E. M. A., Habib, M. A., Ghoniem, A. F., 2015. Fuel flexibility , stability and emissions in premixed hydrogen-rich gas turbine combustion : Technology , fundamentals , and numerical simulations. Applied Energy 154, 1020–1047.

[50] Tryner, J., Tillotson, J. W., Baumgardner, M. E., Mohr, J. T., Defoort, M. W., Marchese, A. J., Mohr, T., Defoort, M. W., Marchese, A. J., 2016. The Effects of Air Flow Rates, Secondary Air Inlet Geometry, Fuel Type, and Operating Mode on the Performance of Gasifier Cookstoves. Environmental Science and Technology 50 (17), 9754–9763.

[51] Tryner, J., Willson, B. D., Marchese, A. J., 2014. The effects of fuel type and stove design on emissions and efficiency of natural-draft semi-gasifier biomass cookstoves. Energy for Sustainable Development 23, 99–109.

[52] Urmee, T., Gyamfi, S., may 2014. A review of improved Cookstove technologies and programs. Renewable and Sustainable Energy Reviews 33, 625–635.

[53] U.S. Department of Energy, 2011. Biomass Cookstoves Technical Meeting: Summary Report.

[54] Varunkumar, S., Rajan, N. K. S., Mukunda, H. S., 2011. Single Particle and Packed Bed Combustion in Modern Gasifier Stoves - Density Effects. Combustion Science and Technology 183 (11), 1147–1163.

[55] Varunkumar, S., Rajan, N. K. S., Mukunda, H. S., 2012. Experimental and computational studies on a gasifier based stove. Energy Conversion and Management 53 (1), 135–141.

[56] Varunkumar, S., Rajan, N. K. S., Mukunda, H. S., 2013. Universal Flame Propagation Behavior in Packed Bed of Biomass. Combustion Science and Technology 185 (8), 1241–1260.

[57] Vassilev, S. V., Baxter, D., Andersen, L. K., Vassileva, C. G., Morgan, T. J., 2012. An overview of the organic and inorganic phase composition of biomass. Fuel 94, 1–33.

[58] Vassilev, S. V., Baxter, D., Vassileva, C. G., 2013. An overview of the behaviour of biomass during combustion: Part I. Phase-mineral transformations of organic and inorganic matter. Fuel 112, 391–449.

[59] Venkataraman, C., Rao, G. U. M., 2001. Emission factors of carbon monoxide and size-resolved aerosols from biofuel combustion. Environmental Science and Technology 35 (10), 2100–2107.

[60] Waldheim, L. Nilsson, T., 2001. Heating value of gases from biomass gasification. IEA Bioenergy Agreement, Task 20 - Thermal Gasification of Biomass, 61.

[61] Wang, G., Silva, R. B., Azevedo, J. L., Martins-Dias, S., Costa, M., 2014. Evaluation of the combustion behaviour and ash characteristics of biomass waste derived fuels, pine and coal in a drop tube furnace. Fuel 117 (PART A), 809–824.

[62] Weber, K., Quicker, P., 2018. Properties of biochar. Fuel 217, 240–261.

[63] Yevich, R., Logan, J. A., 2003. An assessment of biofuel use and burning of agricultural waste in the developing world. Global Biogeochemical Cycles 17 (4), 6.1–6.21.

Highlights:

- Thermochemical conversion of wood, wheat straw and sheep and cow manure was performed.
- Fuel consumption in reverse downdraft process exhibits dependence on the ash content.
- The cold gas efficiency scales linearly from 24–54 % with the process temperature.
- Produced biochars are of high quality for soil amendment purposes.
- Limited the air supply enables efficient production of producer gas and biochar.